

Fracture Conductivity Effect in DFN Modelling Using Carbonate Outcrop Data

Faisal Awad ALJUBOORI ^{a,1}, Jang Hyun LEE ^b Khaled A. ELRAIES ^b
Karl D. STEPHEN ^c Faraj ALSULAIMAN ^a

^a*North Oil Company, Ministry of Oil, Kirkuk 36001, Iraq*

^b*Universiti Teknologi PETRONAS, 32610 Seri Iskandar,
Perak Darul Ridzuan, Malaysia*

^c*Institute of GeoEnergy Engineering, Heriot-Watt University,
Edinburgh EH14 4AS, United Kingdom*

ORCID ID: Faisal Awad ALJUBOORI <https://orcid.org/0000-0002-3659-2744>

Abstract. Synthetic well testing is an important tool which can be utilised to understand the fractures' influence on flow behaviour. Different fracture sets have been used to identify the well performance and the conductivity of the fracture network. Five models were built using outcrop fracture data sets with similar statistical properties, and their flow performances were analysed using the well-test response to evaluate the outcrop-related uncertainties.

The results of the aforementioned scenarios have shown remarkable differences in the pressure responses related to the degrees of fracture conductivity in each fracture set. This variation in the pressure response indicates that the higher fracture density may not necessarily result in a higher fracture conductivity.

The fracture conductivity effect was further investigated using a scenario of a producer completed in a matrix block trapped within fractures. The results have referred that the distance to the fracture and the fracture conductivity have a considerable influence on the dual-porosity signature, which may mask the radial flow response of the matrix in the derivative plot when the fractures are very close.

The outcome of this work can be used to understand the outcrop-related uncertainties as a pre-work of a full field fracture modelling and to calibrate the fracture conductivity at the well vicinity to improve the history matching. The results can also help in well-test interpretations when a similar pattern of pressure response is obtained from real well-test data.

Keywords. Fracture Conductivity, DFN Modelling, Outcrop Modelling, Geological Well Testing, Dual Porosity, Outcrop Statistics

1. Introduction

Naturally Fractured Carbonate Reservoirs are the most challenging reservoirs in terms of management and development [1,2]. The system complexity is related to the multiscale heterogeneity of carbonate rocks, and the later deformation process [3,4,5,6,7,8]. Moreover, the multiscale fractures increase the system complexity and cause the fluid flow behaviour to be significantly varied [9,10,11].

¹Corresponding Author: ALJUBOORI Faisal Awad, f.a.aljuboori@gmail.com

The two types of heterogeneities (fractures and the carbonate matrix) should be characterised accurately in the modelling workflow to enhance the reliability of the reservoir's performance prediction. Moreover, due to the scarcity of fracture data from field measurements [12,13,14] and their usage limitation [14], outcrop analogues are widely used as an alternative source of the required data for fracture modelling. In addition, outcrop studies can help in understanding the subsurface fracture characteristics [13,15] and related uncertainties [16]. New technology has also enhanced the usage of outcrop analogues such as using drones to digitize fractures [14]. Using this technique has accelerated the process of acquiring fracture data with more accuracy [17], and reaching locations that are difficult to access.

The well-test analysis is an essential mean that can be utilised to estimate the reservoir properties and fracture characteristics in dynamic conditions. The well-test response in NFRs has a distinguished signature due to the high contrast between the matrix storativity and transmissivity compared to the fractures, and its interpretation is quite different [18]. The numerical simulation of geological well testing helps to interpret a heterogeneous system that cannot be solved analytically [19,20,21], to evaluate the effect of fracture conductivity on the subsurface pressure behaviour and well productivity, in addition, to assist history matching.

In the current work, the related uncertainties of outcrop-based models have been highlighted by using multiple sets of outcrop fractures and they have been modelled deterministically in multiple models for evaluation purposes. Although the modelled fracture datasets of the outcrop have similar statistical properties, significant differences were obtained. These differences highlight the local variations in the fracture characteristics of each outcrop part, especially the fractures' connectivity in the fracture network (percolation theory), and whether they are connected to the wellbore of the producer. Moreover, the uncertainty evaluation of the outcrop fracture datasets can help in the tuning of the history-matching process to match the well performance and calibrate the reservoir behaviour.

2. Outcrop Description

Outcrop fracture data of a carbonate environment have been employed to simulate the subsurface fluid flow behaviour of fractured carbonate reservoirs [17,22,23]. The analogue area is located in central Tunisia, in the Gafsa Basin, **Figure 1**. It represents the fractured Eocene Carbonate of the Kef Eddour formation. Thousands of fractures, veins and stylolites have been digitised using a camera mounted on a drone to extract fracture data [24], as illustrated in **Figure 2**. Where the outcrop images were processed to interpret the fracture networks to use them in the modelling workflow (e.g.[14,25]). Then the digitised fractures could be preserved in the reservoir simulation [5,23].

Outcrop observations have indicated that two sets of fractures exist, organized into two groups of perpendicular to bedding conjugate system, **Figure 3**, each set containing two orientation families separated by a less than 40° angle [24]. In addition to that, the fracture sets were found to be limited in some distinct bed boundaries such as limestone beds separated by very thin layers (in centimetres) of shale [24]. Moreover, the second fracture set (E-NE to W-SW) has been interpreted as younger because it terminated against the (N-NW to S-SE) fracture set [24].

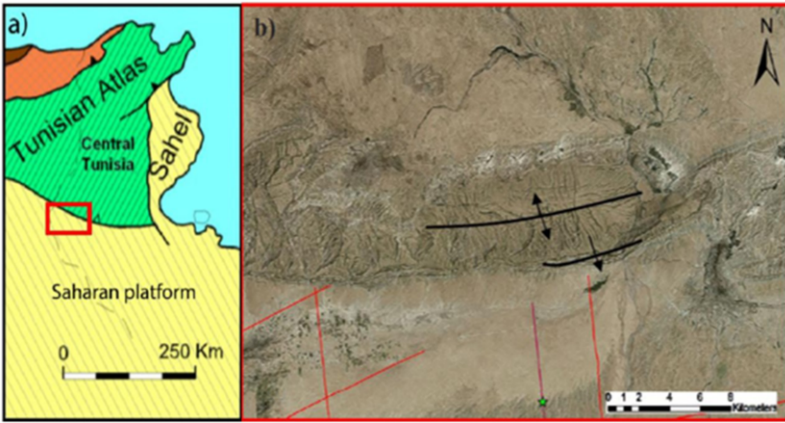


Figure 1. Location of the outcrop data set (a) Setting of Gafsa basin (b) Enlargement of the red box area in (a) with the Alima anticline in the centre. Seismic lines are indicated in red. The green star indicates a well [24]

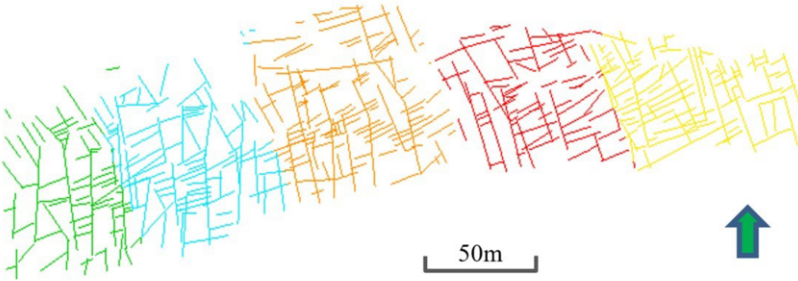


Figure 2. The original outcrop dataset has been modified (coloured) referring to the fracture sub-sets (Set P1 to Set P5, from left to right) that were used to build the simulation models, after [17].

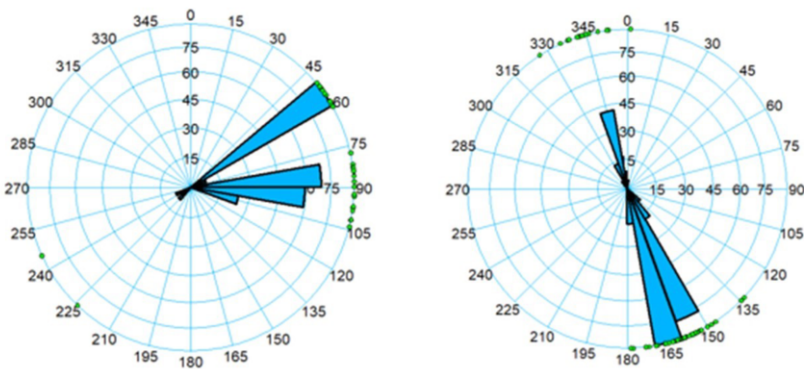


Figure 3. Stereonet plots with Rose Diagrams of the two sets (Set P1 (left) and Set P2 (right)) of fractures, in each diagram, two orientation families separated by less than 40° angle; the green dots refer to the fracture dip with 90° .

3. Model Input Data and Initialization

Five small grid models of dimensions (100m × 100m × 4m) have been built with a resolution of (1m × 1m × 0.5m) in the X, Y, and Z directions respectively, as shown in **Figure 4**. This fine model provides a suitable grid size [25,26] for well testing simulation, improve calculation [27], and to avoid any artefact due to numerical error in the pressure response or pressure derivative [19]. The matrix properties have been set to a constant value of (0.21) for porosity (ϕ_m), and (5mD) for permeability (k_m) to reduce the heterogeneity of the model, and focus on capturing the fractures' behaviour and their performance in the grid models.

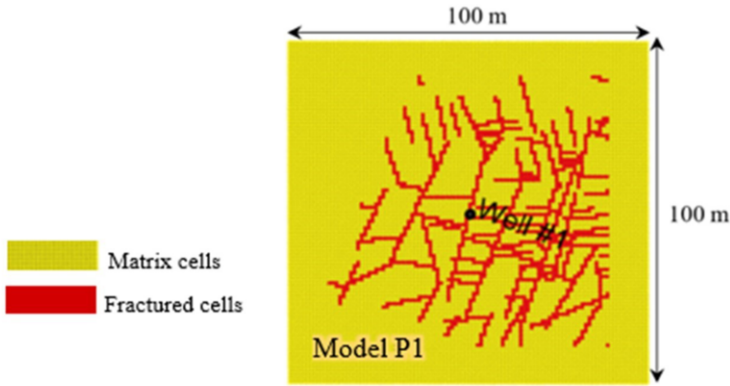


Figure 4. Grid dimensions

Meanwhile, the fracture properties varied depending on the assumption of the aperture size. The fracture permeability, for example, is ranged from 133 Darcy (corresponding to 0.04 mm aperture) to 20,833 Darcy (corresponding to 0.5 mm aperture), as detailed in **Table 1**.

Table 1. Calculated fracture permeability based on the aperture size using the cubic law.

Proposed Cases	Aperture (mm)	Fracture Permeability (D)
A	0.04	133
B	0.1	833
C	0.2	3,333
D	0.3	7,500
E	0.4	13,333
F	0.5	20,833

The illustrated fracture permeability in **Table 1** has been calculated using the widely used formula of cubic law (Parallel Plate Model) as given in **Equation 1** (e.g. [5,17,28,29,30,31]). Furthermore, these high permeability values will be significantly reduced when upscaled to the grid model.

$$Fracture\ Permeability\ (m^2) = \frac{Aperture\ (m)^2}{12} \quad (1)$$

The highlighted fracture sub-sets, in **Figure 2**, were modelled vertically in the grids (dip angle is 90° as observed in the outcrop) using the Discrete Fracture Networks (DFN) approach. The DFN approach has widely been used in modelling fractures (e.g. [32,33, 34,35,36]), which is appropriate for well scale modelling [37]. The fracture sub-sets have honoured detailed geological observations of the outcrop [9]. A summary of fracture length statistics of each fracture sub-sets has listed in **Table 2**.

Table 2. Statistics of fractures length

Parameters	Set P1	Set P2	Set P3	Set P4	Set P5
Mean, m	11.7	12.29	11.19	11.55	11.14
Standard Deviation	8.93	7.73	8.68	8.22	8.25
SD error mean	0.90	0.73	0.80	0.82	0.83
Upper 95% mean	12.86	13.73	12.76	13.18	12.80
Lower 95% mean	9.29	10.85	9.61	9.93	9.49
N	99	113	119	101	98

Real fluid properties of a carbonate reservoir have been adapted in model initialization to ensure realistic reservoir conditions and fluid composition. A synthetic producer was located at the grid centre, and a flow test was designed to maintain the bottom hole flowing pressure above the bubble point pressure to avoid two-phase flow into the wellbore and affect the interpreted permeability value. Further properties of each fracture network such as fracture density and orientation were summarised in **Table 3**.

Table 3. Sub-sets fracture network properties

Parameters	Set P1	Set P2	Set P3	Set P4	Set P5
Cumulative Length, m	1096.35	1388.79	1331.29	1166.78	1092.06
Density (m/m ²)	0.1713	0.2170	0.2080	0.1823	0.1706
Orientation, General	E-NE to W-SW (Set #1); N-NW to S-SE (Set #2)				

The fracture density was calculated using the formula in **Equation 1** [38]. The fracture density will be used for the result comparison. Moreover, these statistics (length, orientation and density) could be used effectively in stochastic fracture modelling [39].

$$\text{Areal Fracture Density } (A_{fD}) = \frac{\text{Cumulative Length } (l_T)}{\text{Bulk Area } (S_B)} \quad (2)$$

4. Results

4.1. The variation in fracture network conductivity

Six proposed scenarios for each grid were examined. The producer in each model was put on stream to propagate a pressure disturbance. Then, the well-test interpretation technique of the derivative plot was employed to determine the pressure response. Remarkable differences in the pressure response and its derivative were observed, which produced a variation in the interpreted permeability and reflected the variation in fracture conductivity in each fracture sub-set. These differences can be illustrated by plotting the interpreted permeability against the input permeability, see **Figure 5**.

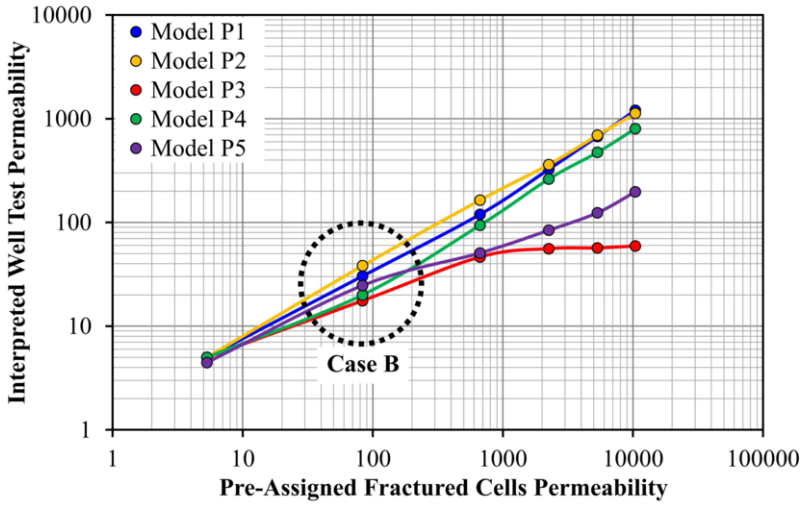


Figure 5. The interpreted system permeability of the five models (P1 to P5).

The differences in pressure response and its derivative in the five models have been illustrated in Figure 6, which shows an example of Case B of the five grids as circled in Figure 5. The pressure derivative has shown that the plateau of each grid is different, which reflects the system radial flow after the dual porosity effect. Then, all the derivative plots converged at the late-time region due to the effect of the closed boundary. The pressure derivative has another advantage of identifying the variation in multiple fracture sets conductivity when they are poorly connected, see Figure 7 and Figure 8.

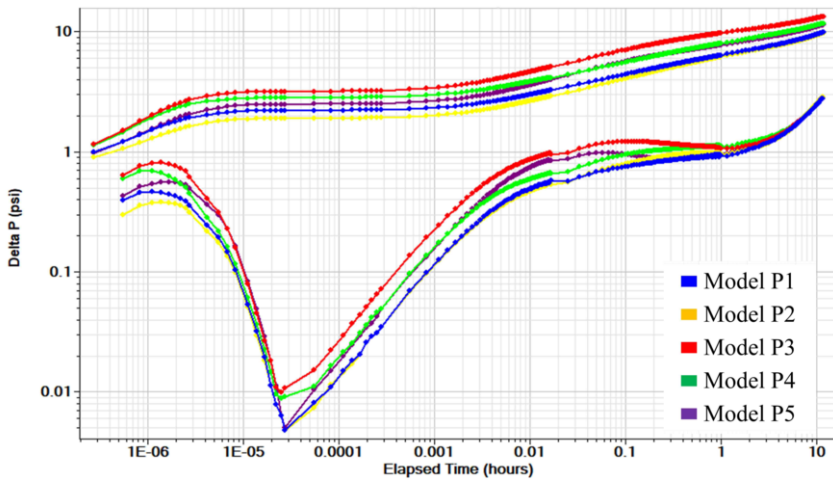


Figure 6. An example of the pressure response and its derivative of Case B for the five models, as shown in a black dotted circle in Figure 5.

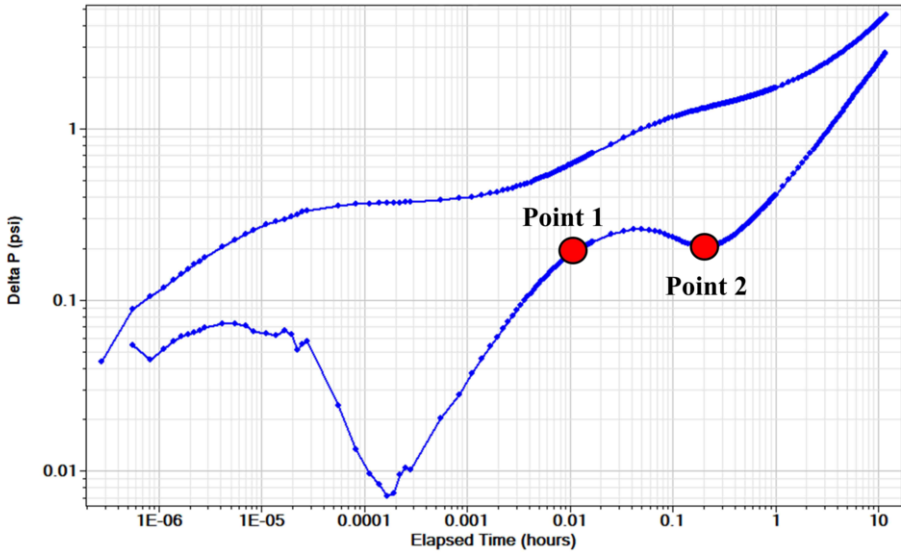


Figure 7. Pressure response and its derivative, identifying two dual porosity signatures in the derivative, which refers to two poorly connected fracture sets.

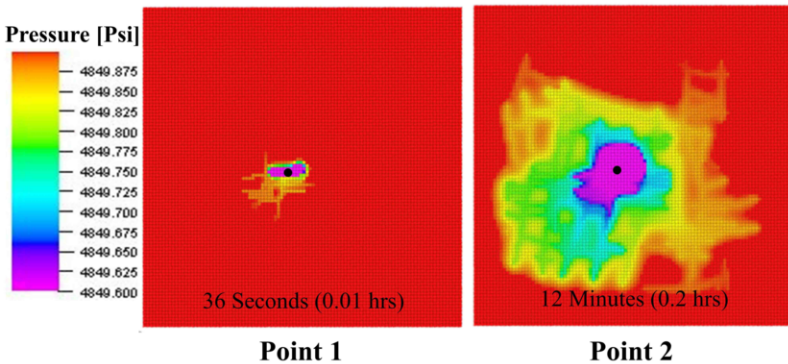


Figure 8. The pressure response in the grid at the end of the first dual porosity signature (point 1 in **Figure 7**) and the second developed dual porosity signature of the second fracture set signature (point 2 in **Figure 7**), represented by light yellow colour at the boundary of the well-drained area.

Further conductivity testing has been done by opening the producers to flow in the five grids for 24 hours. The production constraints were 1000 bbl/D of oil production rate and 2000 psi as the lower limit for the bottom hole pressure. The results are shown in **Figure 9**, **Figure 10**, and **Figure 11**. Moreover, the fractured system behaviour became almost equivalent to a homogeneous system at large times [40], as illustrated in **Figure 11**, Model P1 as an example. Where the effective drainage area (well or field) depends on the opened fractures [13,41], and when the fracture network is well developed [42].

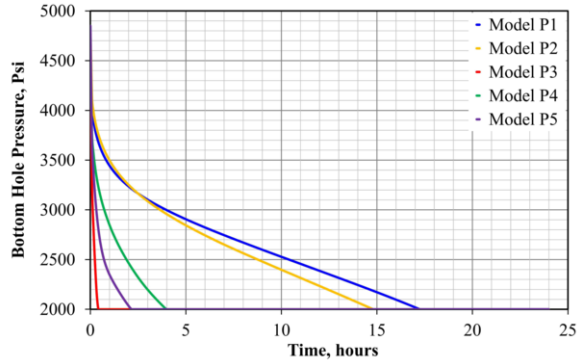


Figure 9. Bottom hole pressure response of the producers in the five models (P1 to P5).

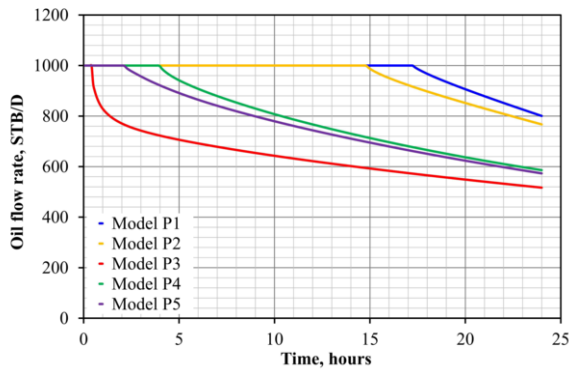


Figure 10. Production rate for 24 hours from the producers of the five models (P1 to P5).

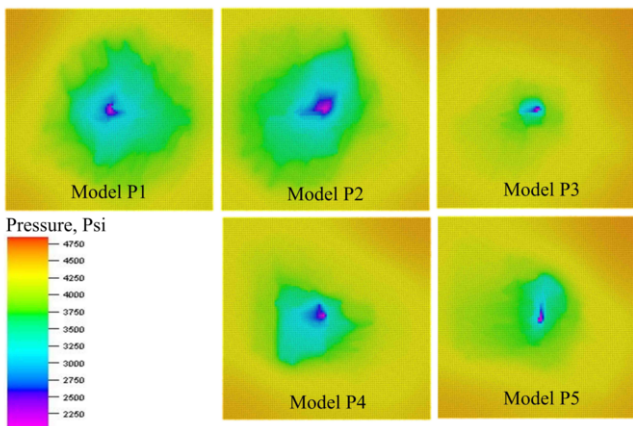


Figure 11. Pressure distribution in the grids after 24 hours of flow, the variation in pressure drainage pattern related to the differences in fracture network conductivity.

4.2. The effect of fracture conductivity on the matrix

In fractured reservoirs, the well trajectory is very important [43]. The productivity and fluid flow behaviour changes dramatically if the producer intersects a fracture or fracture network [17]. The infinite acting behaviour of the dual porosity system indicate by the half slope (linear flow) [44,45], which occurs in a very short time of 10^{-9} to 10^{-6} hours compared to a zero slope line of homogeneous radial flow at 0.01 to 1 hours when the producer completed in the matrix, **Figure 12**.

Moreover, the distinctive signature of the dual porosity (V-shape) appears in the derivative plot also when the producer completed in the matrix only. The appearance time of the dual porosity signature depends on the distance between the producer and the fractures, where the closer the fracture network, the earlier the appearance of the V-shape and the lower value of (ω) (*the ratio of fracture storage to the total system storage*), see **Figure 12**.

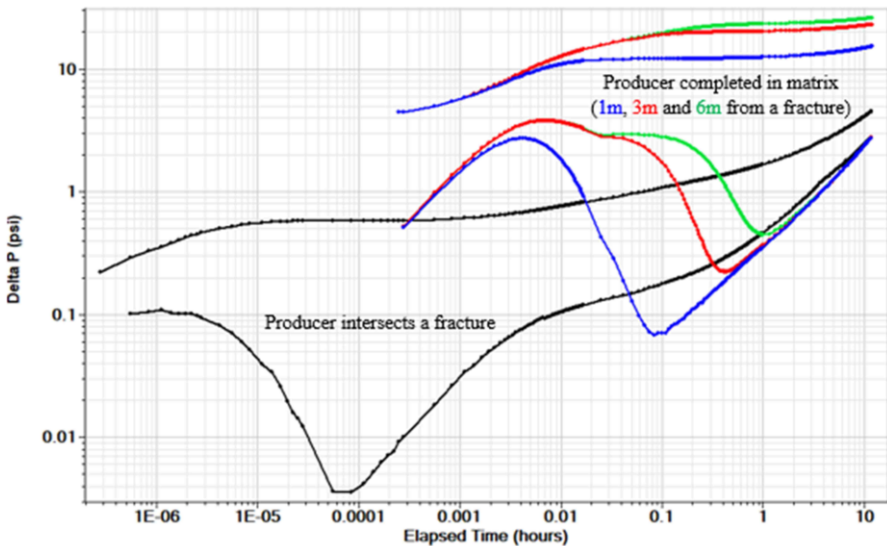


Figure 12. Pressure response and pressure derivative when the producer intersected a fracture (black) and when it completed in a matrix trapped by fractures (blue, red and green).

Different distances between the producer and fracture network were investigated to obtain the pressure response and its derivative in each case, see **Figure 13**. The derivative plot showed that, when the fracture is very close to the producer, the dual porosity effect interfered and masked the radial flow in the matrix (pressure response and its derivative in blue colour represent a 1m distance to the fracture). Moreover, the far distance of the fracture the clearer the radial flow appeared in the derivative plot and the higher (ω) value (*pressure response and pressure derivative in the green colour represent a 6m distance to the fracture*).

For a constant distance of the fracture network from the producer, the variation in fracture conductivity will turn into a variation in (ω) only due to the change in the storage capacity, **Figure 14**.

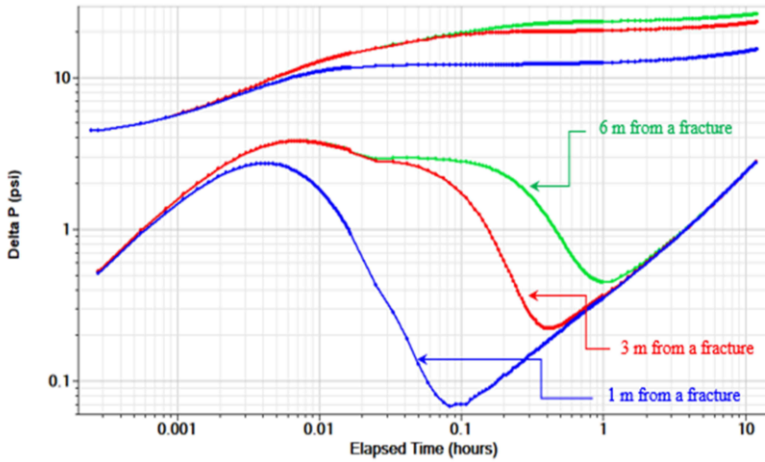


Figure 13. Pressure response and pressure derivative showing the effect of the distance between the producer and the fractures on the dual porosity signature in the derivative plot.

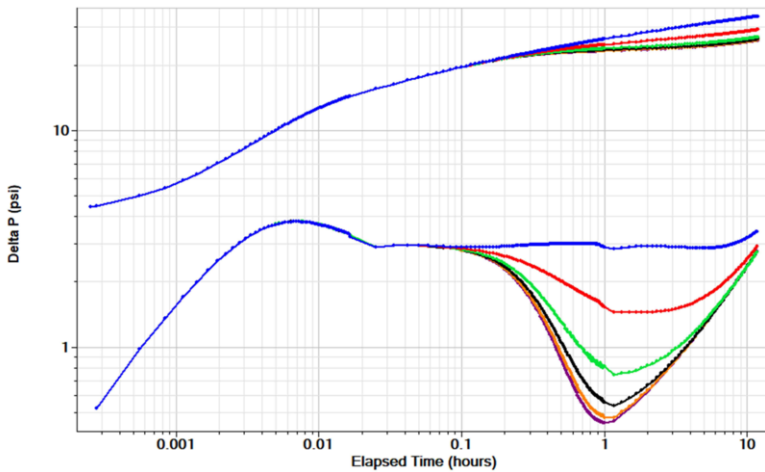


Figure 14. A fracture network located at a 6m distance from a producer completed in the matrix, the decreasing in (ω) value (deeper V shape) related to the increase of the contrast between the storativity of fracture network and matrix.

5. Discussion

The fracture conductivity effect was investigated through outcrop-based models. The pressure drops pattern of the producers depended on the degree of fracture conductivity in each grid and their ability to percolate. In addition to that, fracture density could be a weak indicator for the conductivity of the fracture network (*for example, Model P1 and Model P3*). Although all the producers have completed and produced from fractures, their productivity and fluid flow behaviour are notably different. Therefore, the fracture conductivity remains a calibrating parameter in the matching process [39].

The fracture conductivity effect could be observed also in a pressure response of a producer completed in the matrix. Where the dual porosity signature in the derivative plot may appear after the wellbore storage effect, or in the middle time region depends on the distance to the nearest fracture network. Moreover, if the fracture network is very far from the producer, its effect may be lumped with the boundary effect.

Occasionally, the derivative response is non-unique and further information is necessary to interpret the well test response. In **Figure 7** for example, two (**V**) shapes were obtained in the derivative plot. Although the second (**V**) shape is not well developed due to the boundary effect, it was interpreted as two fracture networks poorly connected. However, this response is similar to what has been produced by Corbett et. al. [5] and they called it the (**W**) shape, which is a response of multiple porosity systems such as fissures, and vugs in addition to fractures.

Furthermore, it is important to consider some important parameters during model setup and initialization such as grid size, retarding the boundary effect by adding matrix cell jacket to the grid boundary [17], real fluid model and rock properties to avoid any modelling artefact due to numerical dispersion and to obtain a realistic well response. Moreover, the outcrop data has provided invaluable data not only for deterministic fracture modelling but also for stochastic fracture modelling (e.g. [46]).

In summary, the current work has highlighted critical issues in fracture modelling workflow using outcrop data such as:

1. Understanding the uncertainties related to the deterministic or stochastic modelling of the fracture analogue data and the possible range of results that could be obtained.
2. Using well test results to adjust the fracture network conductivity within the well drainage area to calibrate the well permeability and to obtain history matching instead of using global multipliers without reasonable justification.

Moreover, the results of the work can help to understand the well-test interpretation when a similar pattern is obtained. The double (**V**) shape and dual porosity signature in the derivative plot have often overlapped with the zero slope line (i.e. the radial flow in the middle-time region), which indicates nearby fractures. Meanwhile, the distal fractures effect may not be obvious in the derivative plot and could be masked by the boundary effect in the late-time region.

6. Conclusions

The results have emphasised the impact of fracture conductivity on well productivity and fluid flow behaviour. Although the modelled fracture sub-sets in this work have comparable statistical properties, their conductivities were varied. The well-developed fracture network has the advantage of draining the adjacent matrix medium and improving oil recovery. Moreover, the results have proven that the higher fracture density may not necessarily lead to a higher fracture conductivity, as it is related to their ability to percolate.

This work has shown that using outcrop-based models has resulted in a series of fracture responses that can be generated for a matrix-fracture system. The classical response of double porosity signature can be seen as parts of a more general response of fractured reservoirs whether the producer intersects with a fracture or not. Moreover, the

dual porosity signature can still be noticed in a producer completed in a trapped matrix block surrounded by a fracture network, and its appearance time is related to the distance between the wellbore and fractures.

History matching could be achieved faster when calibrating the model on a well-to-well basis using the well-test interpretation results. In addition to having a clear understanding of outcrop-based models and their related uncertainties, besides proposing sufficient scenarios to cover the possible range of fluid flow behaviour in the fracture network.

7. Future work

The current work could be extended into two directions; either by focusing on the matrix interactions with the fracture networks or, the ability to obtain a similar behaviour when using the outcrop fracture data deterministically or stochastically, as shown below: -

1. Evaluating the fracture network behaviour and changes in conductivity due to real permeability distribution in the matrix cells of the model instead of a single value.
2. Ability to use the statistical data of the outcrop fractures in building stochastic models of the fracture network, and how the results could be different from the deterministic modelling of the same outcrop fracture by applying the same scenarios.

References

- [1] Richard O. Baker and Frank Kuppe. *SPE-63286-MS*, chapter Reservoir Characterization for Naturally Fractured Reservoirs, page 11. Society of Petroleum Engineers, Dallas, Texas, 2000.
- [2] Faisal Awad Aljuboori, Jang Hyun Lee, Khaled A. Elraies, and Karl D. Stephen. The effectiveness of low salinity waterflooding in naturally fractured reservoirs. *Journal of Petroleum Science and Engineering*, 191:107167, 2020.
- [3] G. Guo and R. D. Evans. *SPE-27025-MS*, chapter Geologic and Stochastic Characterization of Naturally Fractured Reservoirs, page 13. Society of Petroleum Engineers, Buenos Aires, Argentina, 1994.
- [4] Vivian Kay Bust, Joshua Uzezi Oletu, and Paul Francis Worthington. *IPTC-13772-MS*, chapter The Challenges for Carbonate Petrophysics in Petroleum Resource Estimation, page 14. International Petroleum Technology Conference, Doha, Qatar, 2009.
- [5] Patrick WM Corbett, Sebastian Geiger-Boschung, Lindemberg Pinheiro Borges, Mikayil Garayev, Julio Gabriel Gonzalez, Camilo Valdez, et al. Limitations in numerical well test modelling of fractured carbonate rocks. In *SPE EUROPEC/EAGE Annual Conference and Exhibition*. Society of Petroleum Engineers, 2010.
- [6] Viswa Santhi Chandra, Sebastian Geiger, Patrick Corbett, Richard Steele, Paul Milroy, Andrew Barnett, and Paul Victor Wright. *SPE-166033-MS*, chapter Using Near Wellbore Upscaling to Improve Reservoir Characterisation and Simulation in Highly Heterogeneous Carbonate Reservoirs, page 14. Society of Petroleum Engineers, Abu Dhabi, UAE, 2013.
- [7] *High-Resolution Numerical Simulations of Capillary Trapping for Carbon Dioxide in Fractured Formations*, volume All Days of *SPE Reservoir Characterisation and Simulation Conference and Exhibition*, 09 2013. SPE-166002-MS.
- [8] *Uncertainty Quantification for Foam Flooding in Fractured Carbonate Reservoirs*, volume Day 2 Tue, February 21, 2017 of *SPE Reservoir Simulation Conference*, 02 2017. D021S011R007.
- [9] Simeon Agada, Sebastian Geiger, and Florian Doster. Wettability, hysteresis and fracture–matrix interaction during co₂ eor and storage in fractured carbonate reservoirs. *International Journal of Greenhouse Gas Control*, 46:57–75, 2016.

- [10] *A New Methodology to Estimate Fracture Intensity Index for Naturally Fractured Reservoirs*, volume All Days of SPE Western Regional Meeting, 03 2004. SPE-86935-MS.
- [11] Ahmad Sami Abushaikha and Olivier R. Gosselin. *SPE-113890-MS*, chapter Matrix-Fracture Transfer Function in Dual-Media Flow Simulation: Review, Comparison and Validation, page 25. Society of Petroleum Engineers, Rome, Italy, 2008.
- [12] B D M Gauthier, M Garcia, and J M Daniel. Integrated Fractured Reservoir Characterization: A Case Study in a North Africa Field. *SPE-79105-PA*, 2002.
- [13] O P Wennberg, M Azizzadeh, A A M Aqrabi, E Blanc, P Brockbank, K B Lyslo, N Pickard, L D Salem, and T Svana. The Khaviz Anticline: an outcrop analogue to giant fractured Asmari Formation reservoirs in SW Iran. In *Fractured Reservoirs*, volume Special Pu, chapter Outcrop St, pages 23–42. The Geological Society, London, 2007.
- [14] Kevin Bisdom, Giovanni Bertotti, and Hamidreza M Nick. A geometrically based method for predicting stress-induced fracture aperture and flow in discrete fracture networks. *AAPG Bulletin*, 100.
- [15] Ben J. Stephenson, Anton Koopman, Heiko Hillgartner, Harry McQuillan, Stephen Bourne, Jon J. Noad, and Keith Rawnsley. Structural and stratigraphic controls on fold-related fracturing in the zagros mountains, iran: implications for reservoir development. *Geological Society, London, Special Publications*, 270(1):1–21, 2007.
- [16] Beliveau Dennis. Heterogeneity, Geostatistics, Horizontal Wells, and Blackjack Poker. *Journal of Petroleum Technology*, 47(12):1068–1074, 12 1995.
- [17] Faisal Aljuboori, Patrick Corbett, Kevin Bisdom, Giovanni Bertotti, Sebastian Geiger, Kevin Bisdom, and Giovanni Bertotti. Using Outcrop Data for Geological Well Test Modelling in Fractured Reservoirs. Number June 2015, pages 1–4, Madrid, Spain, 1-4 June, 2015.
- [18] J.E. Warren and P.J. Root. The behavior of naturally fractured reservoirs. *Society of Petroleum Engineers Journal*, 3(03):245–255, 09 1963.
- [19] *New Advance in Numerical Well Testing through Streamline Simulation*, volume All Days of SPE Asia Pacific Oil and Gas Conference and Exhibition, 08 2009. SPE-122409-MS.
- [20] *Numerical Well Testing Using Unstructured PEBI Grids*, volume All Days of SPE Middle East Unconventional Resources Conference and Exhibition, 01 2011. SPE-142258-MS.
- [21] G. Stewart. *Well Test Design & Analysis*. PennWell, 2011.
- [22] Kevin Bisdom. Natural fracture patterns in carbonate rocks, 2015.
- [23] Faisal Awad Aljuboori, Jang Hyun Lee, Khaled A. Elraies, and Karl D. Stephen. The impact of diagenesis precipitation on fracture permeability in naturally fractured carbonate reservoirs. *Carbonates and Evaporites*, 36(1):6, Nov 2020.
- [24] K. Bisdom, G. Bertotti, and B.D.M. Gauthier. Predicting multi-scale deformation and fluid flow patterns in folds using 3d outcrop models and mechanical modelling. volume 2014, pages 1–5. European Association of Geoscientists and Engineers, 2014.
- [25] B. J. Bourbiaux, M. C. Cacas, S. Sarda, and J. C. Sabathier. *SPE-38907-MS*, chapter A Fast and Efficient Methodology to Convert Fractured Reservoir Images Into a Dual-Porosity Model, page 12. Society of Petroleum Engineers, San Antonio, Texas, 1997.
- [26] *Numerical Well Testing: A Method to Use Transient Testing Results in Reservoir Simulation*, volume All Days of SPE Annual Technical Conference and Exhibition, 10 2005. SPE-95905-MS.
- [27] J R Gilman and H Kazemi. Improved Calculations for Viscous and Gravity Displacement in Matrix Blocks in Dual-Porosity Simulators . *SPE-16010-PA*, 1988.
- [28] Paul Adams Witherspoon, Joseph SY Wang, K Iwai, and John E Gale. Validity of cubic law for fluid flow in a deformable rock fracture. *Water resources research*, 16.
- [29] Muhammad Sahimi. *Flow and transport in porous media and fractured rock: from classical methods to modern approaches*. John Wiley & Sons, 2011.
- [30] Sebastian Geiger and Stephan Matthäi. What can we learn from high-resolution numerical simulations of single- and multi-phase fluid flow in fractured outcrop analogues? *Geological Society, London, Special Publications*, 374(1):125–144, 2014.
- [31] Pierre M. Adler, Jean-François Thovert, and Valeri V. Mourzenko. *Fractured Porous Media*. Oxford University Press, 10 2012.
- [32] William S. Dershowitz, J Hermanson, S Follin, and M Mauldon. Fracture intensity measures in 1-D, 2-D, and 3-D at Aspo, Sweden. *Pacific Rocks 2000: Rock around the Rim*, 2000.
- [33] *An Integrated Workflow to Account for Multi-Scale Fractures in Reservoir Simulation Models: Implementation and Benefits*, volume All Days of Abu Dhabi International Petroleum Exhibition and Confer-

- ence, 10 2002. SPE-78489-MS.
- [34] H. Kazemi, S. Atan, M. Al-Matrook, J. Dreier, and E. Ozkan. *SPE-93053-MS*, chapter Multilevel Fracture Network Modeling of Naturally Fractured Reservoirs, page 8. Society of Petroleum Engineers, The Woodlands, Texas, 2005.
- [35] *Integrated Reservoir Connectivity Study of Ahmadi Fractured Reservoir in Bahrain Field*, volume All Days of *SPE Middle East Oil and Gas Show and Conference*, 03 2009. SPE-120665-MS.
- [36] *Reduced Order Models for Rapid EOR Simulation in Fractured Carbonate Reservoirs*, volume Day 1 Mon, February 23, 2015 of *SPE Reservoir Simulation Conference*, 02 2015. D012S021R009.
- [37] B D M Gauthier, A M Zellou, A Toublanc, M Garcia, and J M Daniel. Integrated Fractured Reservoir Characterization: a Case Study in a North Africa Field. In *SPE-65118-MS*. Society of Petroleum Engineers, 2000.
- [38] T.D. Van Golf-Racht, editor. *fundamentals of fractured reservoir engineering*, volume 12 of *Developments in Petroleum Science*. Elsevier, 1982.
- [39] J. C. Sabathier, B. J. Bourbiaux, M. C. Cacas, and S. Sarda. *SPE-39825-MS*, chapter A New Approach of Fractured Reservoirs, page 11. Society of Petroleum Engineers, Villahermosa, Mexico, 1998.
- [40] H. Kazemi. Pressure transient analysis of naturally fractured reservoirs with uniform fracture distribution. *Society of Petroleum Engineers Journal*, 9(04):451–462, 1969.
- [41] Luis Guerreiro, Antonio Costa Silva, Victor Alcobia, and Amilcar Soares. Integrated Reservoir Characterisation of a Fractured Carbonate Reservoir. In *SPE-58995-MS*. Society of Petroleum Engineers, 2000.
- [42] C. L. Jensen, S. H. Lee, W. J. Milliken, J. Kamath, W. Narr, H. Wu, and J. P. Davies. *SPE-48999-MS*, chapter Field Simulation of Naturally Fractured Reservoirs Using Effective Permeabilities Derived From Realistic Fracture Characterization, page 14. Society of Petroleum Engineers, New Orleans, Louisiana, 1998.
- [43] Ronald Nelson. *Geologic analysis of naturally fractured reservoirs*. Elsevier, 2nd edition, 2001.
- [44] Dominique Bourdet, editor. *Well Test Analysis: The Use of Advanced Interpretation Models*, volume 3 of *Handbook of Petroleum Exploration and Production*. Elsevier, 2002.
- [45] Roland N Horne. *Modern well test analysis*, volume 1141. Petroway Inc, second edition, 1995.
- [46] Faisal Awad Aljuboori, Jang Hyun Lee, Khaled A Elraies, and Karl D Stephen. Effect of fracture characteristics on history matching in the Qamchuqa reservoir: a case study from Iraq. *Carbonates and Evaporites*, 35(3):87, 2020.